

Petrogenesis of an early Cretaceous potassic lamprophyre dyke from Rongjeng, East Garo Hills, Shillong plateau, north-eastern India

Rajesh K. Srivastava^{1,*}, Leone Melluso² and Anup K. Sinha³

¹Department of Geology, Centre of Advanced Study, Banaras Hindu University, Varanasi 221 005, India

²Dipartimento di Scienze della Terra, dell'Ambiente e delle Risorse, Università di Napoli Federico II, I-80134 Napoli, Italy

³Dr K.S. Krishnan Geomagnetic Research Laboratory, Indian Institute of Geomagnetism, Allahabad 211 505, India

An early Cretaceous potassic lamprophyre dyke, exposed near Rongjeng, East Garo Hills, Shillong plateau, north-eastern India, is a highly porphyritic rock with large phenocrysts of clinopyroxene, phlogopite, amphibole and olivine. Reversely zoned phlogopite and clinopyroxene grains indicate that some degree of interaction between magma batches of variable composition took place somewhere during the crystallization of the lamprophyre. Mineral compositions indicate its derivation from an alkaline magma comparable with those that filled the nearby Jasra potassic intrusion. Moreover, the geochemistry of the Rongjeng lamprophyre is distinctly different from that of the Damodar Valley lamproites, the Sung Valley carbonatitic-ijolitic intrusion, and the Antarctic ultramafic lamprophyres. The contrasting geochemical affinity is suggestive of heterogenous lithospheric mantle sources, rather than input of plume-related magmatism.

Keywords: Geochemistry, lithospheric alkaline magmatism, mantle heterogeneity, petrogenesis, potassic lamprophyre.

LAMPROPHYRE is an alkaline rock that normally contains high alkalis at a given percentage of SiO₂, together with one or more of normative nepheline, leucite or acmite, modal foids, and Na–K–Ti-rich amphiboles, micas or pyroxenes¹. They usually occur as dykes throughout all geologic eras. Many^{2,3} have strictly forbidden the terms like 'lamprophyric rocks', or 'lamprophyre clan' and defined lamprophyre as a porphyritic igneous rock with mafic index between 35 and 90 and contain phenocrysts of biotite/phlogopite, amphibole, clinopyroxene and olivine. Feldspars and/or feldspathoids, if present, are restricted to the groundmass. Calcite and zeolite may be secondary phases. Although lamprophyres are volumetrically insignificant components of continental magmatism, their systematic studies may provide significant information to our understanding of deep melting events during the initial stages of continental rift development^{4,5} or inference a mantle-plume connection^{6,7}.

*For correspondence. (e-mail: rajeshgeolbhu@gmail.com)

The Indian shield comprises a number of lamprophyric occurrences ranging their ages from Precambrian to Cretaceous and varies in compositions from calc-alkaline to ultramafic^{8–11}. Alkaline and mafic dykes of different compositions are reported from the Shillong plateau, north-eastern India¹², however, concentration of these dykes is more in East Garo Hills, particularly around Swangkre, Rongjeng, Nongchram, Rongmil and Darugiri areas^{12–17}. Most of these mafic dykes are Proterozoic in age¹², whereas alkaline and carbonatite dykes, mostly exposed around Swangkre, Rongjeng and Nongchram, are emplaced during early Cretaceous^{15,16}. Nambiar^{15,16} has presented some petrological and major element oxides data on alkaline dykes of this region, however, no other work is available on these rocks. Here we present a detailed account on mineral chemistry and whole-rock geochemistry which includes major, trace and rare-earth element concentrations on an early Cretaceous potassic lamprophyre dyke exposed near Rongjeng, East Garo Hills, Shillong plateau, north-eastern India to understand the petrogenesis and possible role of a mantle plume.

Geological setting

The most spectacular geological feature in north-eastern Indian shield is Shillong plateau which is an uplifted horst-like feature, bounded on all sides by several fault systems such as Dauki, Brahmaputra, Jamuna and Kopili^{18–22} (Figure 1). There are some other deep faults which traverse the Shillong plateau; this includes the N–S trending Nongchram fault and Um Ngot lineaments and NE–SW trending Badapani–Tyrsad shear zone^{14,16,22,23} (Figure 1). It is believed that most of these deep faults/lineaments are developed during the late Jurassic–early Cretaceous and spatially and temporally associated with the early Cretaceous mafic–ultramafic–alkaline igneous magmatism²². The Shillong plateau is mainly formed by (i) Archaean gneisses, (ii) Proterozoic mafic dykes, (iii) Shillong Group of rocks (Proterozoic orthoquartzites and phyllites), (iv) a number of 700–450 Ma granite plutons that intrude the gneissic basement as well as the Shillong Group cover, (v) the Sylhet Traps, a part

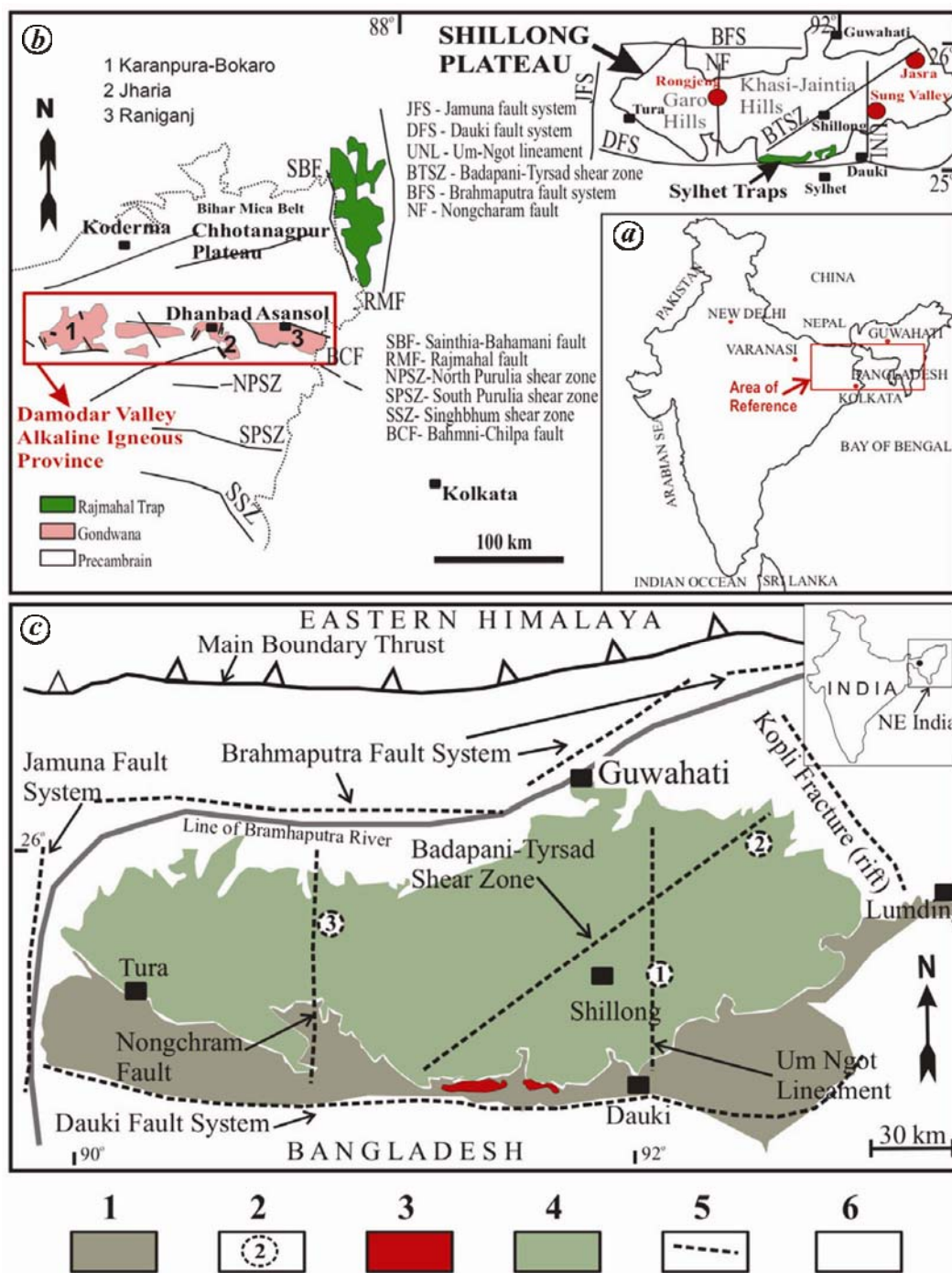


Figure 1. a, Map of India showing area of present study. b, Geological sketch map of northeastern India showing the locations of Cretaceous magmatic activity in the Damodar Valley, Rajmahal and Sylhet Traps and on the Shillong Plateau³⁸. c, Regional geological and tectonic set-up of the Shillong Plateau¹⁸. 1, Cretaceous-Tertiary sediments; 2, Ultramafic-alkaline-carbonatite complexes [(1) Sung Valley; (2) Jasra; (3) Rongjeng-Swangkre]; 3, Sylhet basalts; 4, Archaean-gneissic complex, Shillong Group rocks, mafic igneous rocks, and Proterozoic granites; 5, Major fault-systems, and 6, Alluvium and recent sediments.

of the early Cretaceous Rajmahal-Sylhet flood basalt province, and (vi) the early Cretaceous ultramafic-alkaline-carbonatite complexes^{18,20,23-26} (Figure 1). It is suggested that early Cretaceous magmatism recorded in the Shillong plateau has definite association with the Kerguelen plume²⁷⁻³¹.

A number of early Cretaceous dykes are reported to be emplaced within the Archaean gneissic complex of the Shillong plateau, which includes hornblende and biotite gneisses, porphyritic granitoids and pink granites^{15,16}. Although Nambiar^{15,16} reported dykes of different compositions such as basalt/dolerite, nepheline syenite, lam-

prophyre, ijolite and carbonatite; basalt/dolerite and feldspathic dykes dominate, other lithotypes are rare. Most of these dykes trend N–S and were emplaced parallel to the Nongcharam deep fault^{15,16} (Figure 2). The potassic lamprophyre dyke under study (25°38'19"E: 90°48'31"N) is exposed around Rongjeng area and is an integral part of the Swangkre dyke swarm^{15–17} (Figure 2). It is a small dyke (width varies between 50 cm to 100 cm), trends N–S, and has been emplaced at 107 ± 3 Ma (ref. 32). It is a highly porphyritic rock (Figure 3), with large phenocrysts of clinopyroxene and phlogopite (up to 5 mm in size), with lower amounts of amphibole, olivine and oxides (in order of abundance), with microlites of clinopyroxene, phlogopite, apatite and alkali feldspar. Carbonates, analcime, other zeolites and rutile are secondary minerals. Very frequent and highly distinctive is the presence of reversely zoned phlogopite and clinopyroxene, with cores of Fe-rich, green clinopyroxene and Fe-rich, dark brown phlogopite and distinctly more magnesian (colourless) rims.

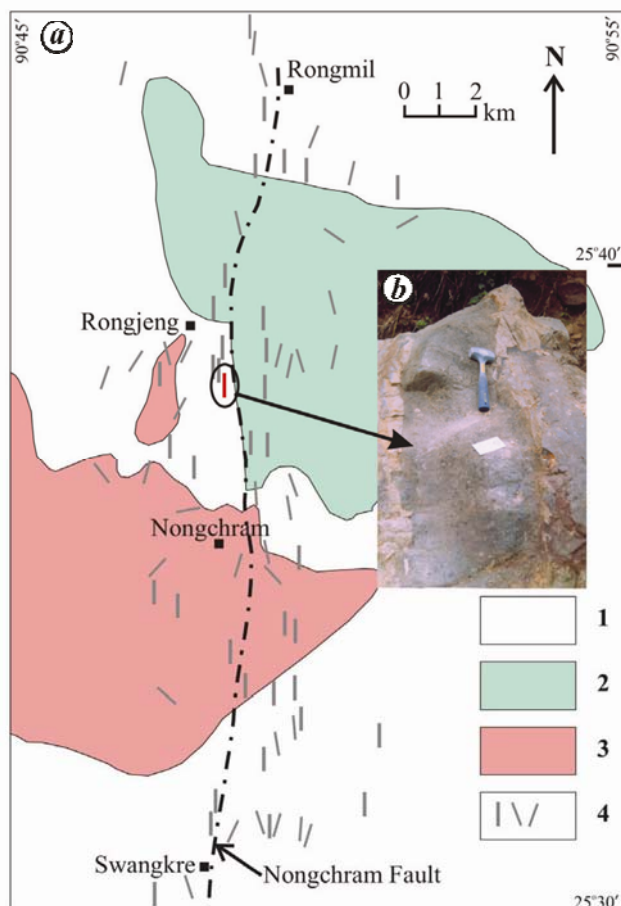


Figure 2. *a*, Simplified geological map of Swangkre-Rongjeng area^{15–17}. (1) Migmatitic gneisses, (2) Porphyritic granite, (3) Pink granite, (4) Dykes of different petrological compositions. Location of studied potassic lamprophyre dyke is encircled. Width and length of dykes are not to scale. *b*, Field photograph of potassic lamprophyre dyke exposed near Rongjeng.

Mineral compositions

Mineral analyses, obtained with energy dispersive spectrometry (EDS), have been performed at CISAG, University of Napoli Federico II, utilizing an Oxford Instruments Microanalysis Unit, equipped with an INCA X-act detector and a JEOL JSM-5310 microscope operating at 15 kV primary beam voltage, 50–100 mA filament current, and 50 s net acquisition time. Measurements were done with an INCA X-stream pulse processor. The following standards were used for calibration: diopside (Mg), wollastonite (Ca), anorthoclase (Al, Si), albite (Na), rutile (Ti), almandine (Fe), Cr₂O₃ (Cr), rhodonite (Mn), orthoclase (K), apatite (P), fluorite (F), barite (Ba), strontianite (Sr), Smithsonian orthophosphates (REE, Y), pure niobium (Nb), pure vanadium (V), zircon (Zr, Hf), Corning glass (Th and U), sphalerite (S) and sodium chloride (Cl). Table 1 presents representative mineral analyses of different mineral phases; complete analyses (see Supplementary Information Tables S1–S4, online) are available as supplementary material on journal's website.

Olivine

The rare olivine phenocrysts have a composition ranging from Fo₈₅ to Fo₈₁, are low in CaO (CaO from 0.2 to 0.6 wt%) and do not host chromite crystals. Their compositions indicate crystallization from a slightly evolved melt composition, having Mg# from 85 to 81; according to the olivine–liquid Fe–Mg partitioning³³ (see supplementary information, Table S1, online). These values are close to the bulk rock composition of SW02/9, having an Mg# = 67, suggesting near equilibrium.

Clinopyroxene

Two generations of clinopyroxene are observed among phenocrysts and/or cores (see Supplementary Information, Table S2, online; Figure 4). Diopside (Mg# = 70–82) has the marked enrichment in TiO₂ and Al₂O₃ (up to 4 and 9 wt% respectively) with decreasing Mg#, typical of pyroxene crystallizing in within-plate alkaline magmas. Fe-rich clinopyroxene (Mg# 20–70) tends to be rich in Na (up to 5 wt%) and low in TiO₂ and Al₂O₃. This pyroxene also occurs as green cores, likely crystallized in more evolved magma batches.

Phlogopite

Brown mica has also two generations of phenocrysts (see Supplementary Information Table S3, online; Figure 5). Phlogopite has high Mg# (76–83) and TiO₂ up to 5 wt%, whereas Fe-rich varieties (Mg# 33–57) have variable TiO₂ (4.3–5.4 wt%). BaO reaches values as high as

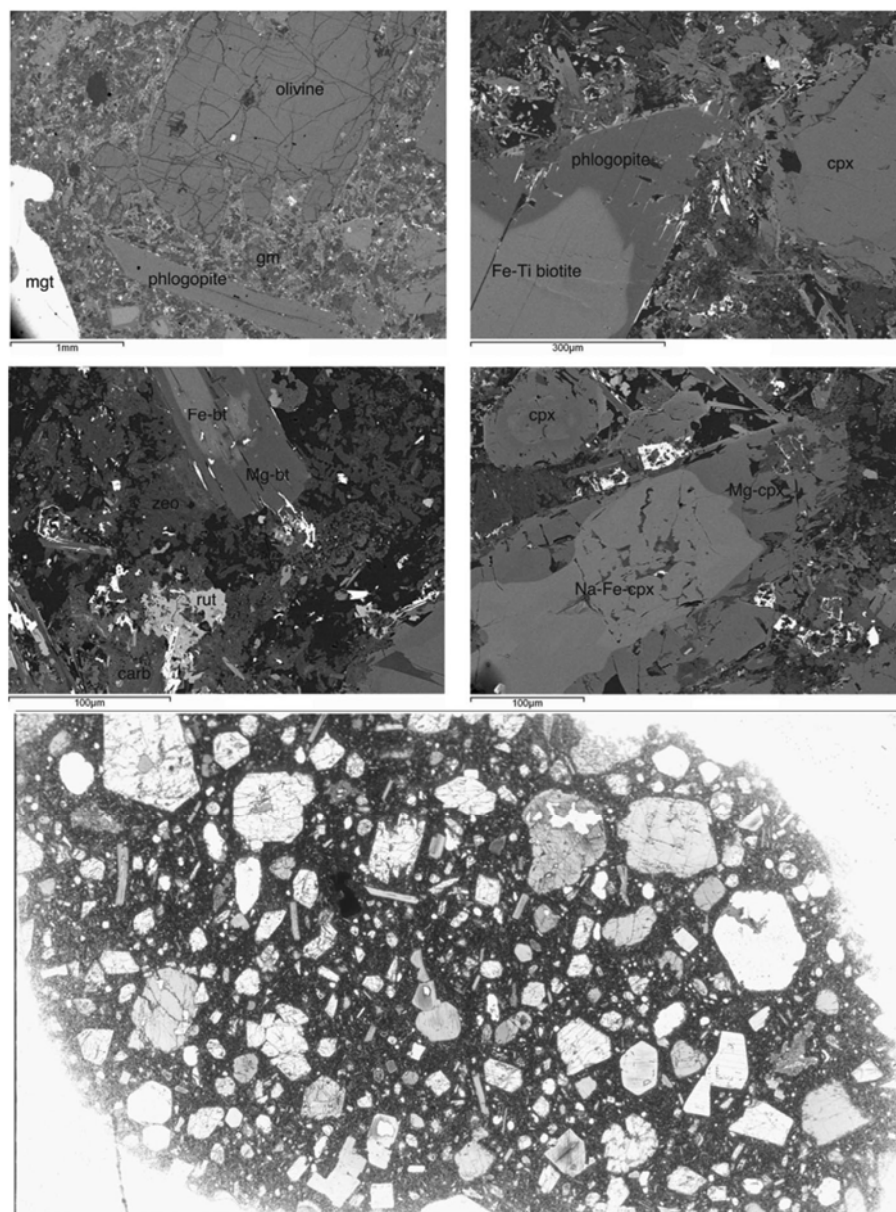


Figure 3. Back-scattered electron and microscope images of peculiar petrographic features of the Rongjeng potassic lamprophyre sample showing porphyritic texture. Phenocrysts of biotite-phlogopite, clinopyroxene and olivine are visible. Fine-grained groundmass is composed of feldspathic minerals, feldspars and biotite. The bottom photograph is polished slab of the studied sample (the long side is about 2.5 cm).

1.3 wt%. The mica compositions are similar to those of the Jasra micas, and very different from those of the Damodar Valley lamproites or those of the Sung Valley carbonatite–jollite complex (Figure 5), thus suggesting a range of different parental magmas.

Amphibole

Amphibole is quite rare as phenocryst, and has pargasitic chemistry (Supplementary Information, Table S4, online; Figure 6), with Mg# from 64 to 71 and TiO₂ reach values as high as 4.9 wt%. The Jasra amphiboles are mostly

kaersutites, hence having slightly more TiO₂ (up to 6.3 wt%).

Other minerals

Rare Ti-magnetite has been found (TiO₂ 10.7–11.2 wt%; ulvöspinel content) and rutile/leucoxene. Pyrite, pyrrhotite and blende are sporadically found in the groundmass. Alkali feldspar has a quite uniform composition (Or_{87–89} Ab_{11–12} An_{0–1}) and tends to be altered to zeolites. Apatite is rare and has F and SO₃. Barite is also sporadically found. Secondary carbonates are sometimes rich in Fe.

Table 1. Representative chemical compositions of different mineral phases in Rongjeng potassic lamprophyre (SW02/9)

	Clinopyroxenes												Micas						Amphiboles													
	Olivines			cpx core			cpx rim			cpx core			cpx rim			phlog mic		phlog core		phlog rim		phlog gm		amph core		amph rim		amph				
SiO ₂	40.49	39.86	48.51	48.71	43.72	43.94	50.04	50.04	36.88	37.15	37.92	37.83	37.26	37.48	37.06	36.47	37.70	40.91	41.33	41.68	39.83											
TiO ₂			1.84	1.53	3.64	3.46	1.68	1.68	4.56	4.22	4.95	4.28	4.26	4.75	4.79	3.71	3.57	3.37	3.56	3.49	3.94											
Al ₂ O ₃			6.59	6.68	8.80	7.70	6.07	16.23	16.23	15.93	16.07	15.35	9.21	13.67	15.86	15.83	15.09	13.16	13.35	13.30	13.31											
FeO	13.61	16.34	5.51	5.03	7.67	7.18	8.30	7.20	8.37	8.37	6.66	9.19	24.94	12.04	6.59	7.60	10.18	11.00	10.25	10.03	10.16											
MnO	0.07	0.29	0.09	0.09	0.00	0.13	0.00	0.13	0.10	0.10	0.10	0.20	0.62	0.32	0.24	0.04	0.02	0.11	0.11	0.07	0.44											
MgO	44.70	43.46	12.88	12.99	11.04	11.66	12.24	18.62	19.06	19.06	18.77	18.16	9.86	16.49	18.64	19.46	18.32	12.95	13.27	13.48	13.43											
CaO	0.25	0.21	23.25	22.94	24.01	23.70	22.31	0.11	0.74	0.66	0.75	0.73	0.26	0.14	0.15	0.08	0.12	11.84	11.37	11.51	11.44											
Na ₂ O			0.70	0.93	0.60	0.73	1.22		0.59	1.18	0.61	0.47	0.78	0.52	0.49	1.17	0.96	0.08	0.14	0.14	0.41											
K ₂ O									9.63	9.49	10.18	10.08	9.80	10.21	9.84	9.01	9.24	2.23	2.12	2.14	2.10											
BaO									0.59	1.18	0.61	0.47	0.78	0.52	0.49	1.17	0.96	0.08	0.14	0.14	0.41											
SrO																																
Cr ₂ O ₃			0.06	0.25	0.11	0.09	0.11		0.05	0.05	0.42			0.30																		
V ₂ O ₅																																
F									0.06	0.24	0.29		0.16	0.10	0.09																	
Cl									0.02	0.08	0.08	0.02	0.08																			
H ₂ O*									4.07	4.03	4.02	4.12	3.73	4.00	4.06	4.05	4.10															
O=F,Cl									0.03	0.10	0.14	0.01	0.08	0.04	0.04	0.00	0.00	0.00	0.00	0.01	0.00											
Total	99.11	100.16	99.43	99.14	99.60	98.59	101.98	98.8	100.7	100.6	100.6	100.4	101.0	100.1	98.6	98.0	100.0	99.98	99.90	100.28	99.74											
Mg#	85	82	80	82	72	74	72	82	80	83	83	78	41	71	83	82	76	68	70	71	71											

Geochemistry

Whole rock major, trace and rare-earth element analysis of the lamprophyre was performed at the Activation Laboratories Ltd, Ancaster, Ontario, Canada. ICP-OES (Model: Thermo-JarretAsh ENVIRO II) was used to analyse major elements, whereas ICP-MS (Model: Perkin Elmer Sciex ELAN 6000) was used to determine trace and rare-earth element concentrations. The precision is <5% for all analysed elements when reported at

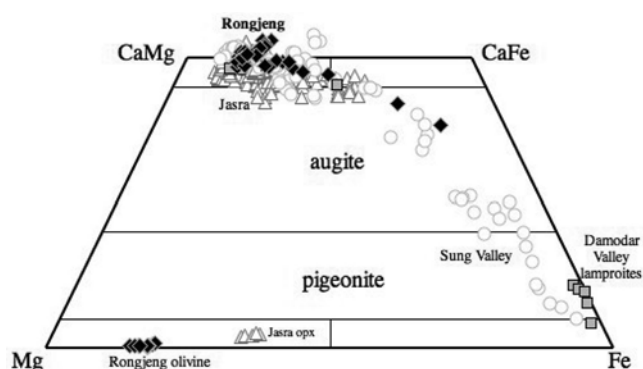


Figure 4. Pyroxene compositions in the Rongjeng potassic lamprophyre plotted on a standard Ca–Mg–(Fe + Mn) ternary diagram (in at%).

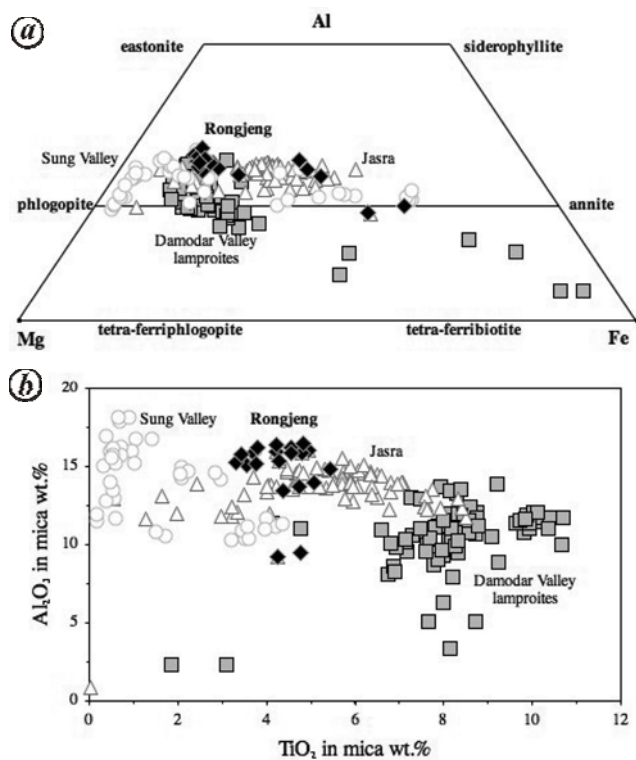


Figure 5. Classification of micas in the Rongjeng potassic lamprophyre. TiO_2 versus Al_2O_3 variation in micas in the Rongjeng potassic lamprophyre.

100 × detection limit. Several standards, such as SY-3, W-2, DNC-1, BIR-1 and STM-1, were run along with the analysed UML sample to check accuracy and precision. Geochemical data is presented in Table 2. Mg number (Mg#) is calculated using the SINCLAS Computer Program³⁴.

Chemical composition of the studied potassic lamprophyre sample shows low-silica, high-magnesium and moderate-alkalis composition. The weight loss on ignition (LOI) is high; due to the carbonate phases. High Mg# indicates its derivation from a mantle-derived melt. On TAS plot³ (Figure 7a), the potassic lamprophyre sample shows basanite composition. The SINCLAS Computer Program³⁴ classifies it as melanephelinite type basanite, which also indicates its melanocratic alkaline nature. Although Rock^{35,36} distinguished ‘alkaline’ from ‘ultramafic’ lamprophyres, it is difficult to differentiate them; both have several overlapping mineralogical and geochemical characteristics. Their overlapping geochemical nature is well observed on Al_2O_3 –CaO–MgO plot¹ (Figure 7b). Nevertheless, it is also true that both lamprophyre types suffered broadly similar petrogenetic histories³⁷.

The Rongjeng dyke has low Cr and Ni concentrations (130 and 100 ppm respectively), indicating that it experienced some degree of fractional crystallization from more primitive compositions. Nonetheless, the high Ba, Sr Nb and Zr concentrations are typical of alkaline-within-plate alkaline magmas. The rare earth element chondrite normalized pattern is steep ($\text{La}/\text{Yb}_N = 22$), and has no negative Eu anomalies, indicating no previous feldspar removal. The mantle normalized incompatible element pattern of the Rongjeng lamprophyre is typical of potassic within-plate mafic rocks. It has a peak at Ba, no K, Nb, Ta and Ti troughs and a substantially smooth pattern towards the least incompatible elements.

Discussion

From the petrography, mineral chemistry and geochemistry, presented above, it can be established that the

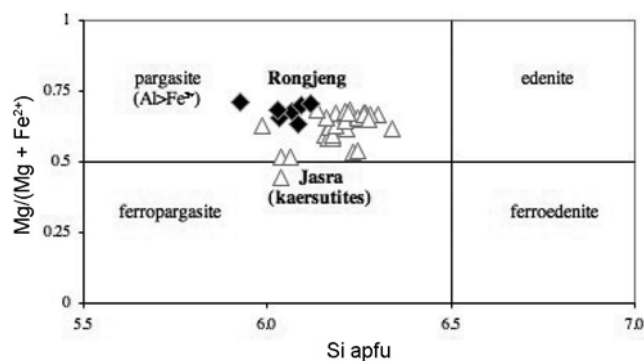
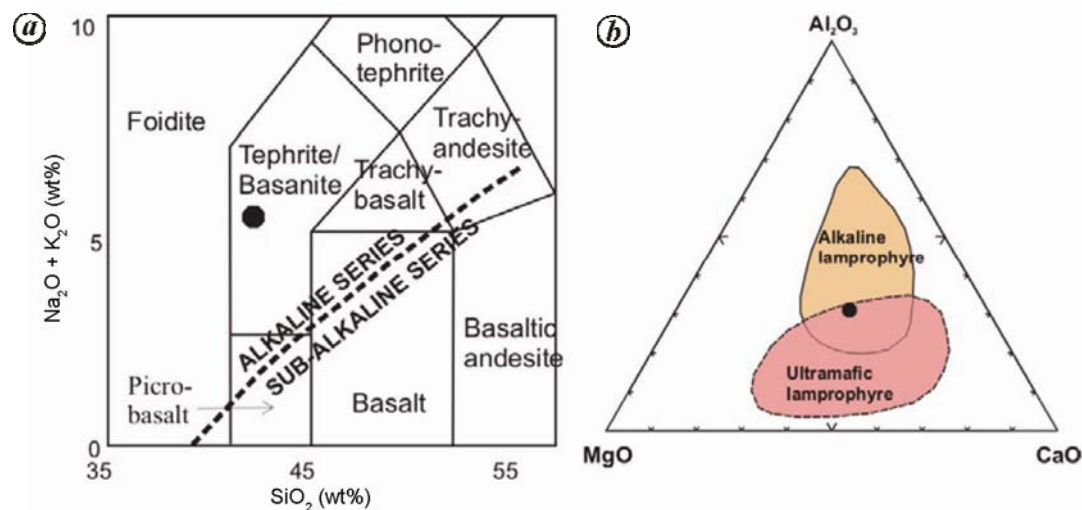


Figure 6. Amphibole compositions in the Rongjeng potassic lamprophyre.

Table 2. Whole rock major, trace and rare-earth element and CIPW normative compositions of potassic lamprophyre (SW02/9) from the Rongjeng, Shillong Plateau NE India

	SiO ₂	TiO ₂	Al ₂ O ₃	Fe ₂ O ₃	MnO	MgO	CaO	Na ₂ O	K ₂ O	P ₂ O ₅	LOI	Total	Mg#	
Major oxides (wt%)	37.42	2.41	10.28	11.15	0.15	10.17	12.76	2.76	2.00	0.63	9.12	98.85	68.07	
Trace elements (ppm)	V	Cr	Ni	Ga	Rb	Sr	Ba	Y	Zr	Hf	Nb	Ta	Th	U
	260	128	102	14	72	744	968	20	192	4.5	47	2.6	4.8	1.0
Rare-earth elements (ppm)	La	Ce	Pr	Nd	Sm	Eu	Gd	Tb	Dy	Ho	Er	Tm	Yb	Lu
	45.00	88.20	9.63	36.20	6.60	2.01	6.00	0.80	3.90	0.70	1.80	0.24	1.50	0.21

**Figure 7.** *a*, Total-alkali and silica diagram³. Dotted line separates sub-alkaline rocks from alkaline rocks⁴². *b*, Al₂O₃–CaO–MgO (wt%) ternary plot for distinguishing alkaline and ultramafic lamprophyres¹.

studied sample has potassic affinity. It mainly contains phenocrysts of clinopyroxene and phlogopite, and minor amounts of amphibole, olivine and oxides are also present in a fine-grained groundmass. Its alkaline nature is also reflected from the geochemical characteristics. The mineral compositions of the lamprophyre are typical of those crystallizing in alkaline magmas and substantially similar to those found in the nearby alkaline intrusions of the Shillong Plateau. The reversely zoned phases indicate that some degree of interaction between magma batches of variable composition took place somewhere during the crystallization of the lamprophyre (Figure 3).

The chemical composition of the main mineral phases of the Rongjeng lamprophyre is close to the range observed in the mafic samples of the nearby Jasra potassic intrusion, thought to be filled by magmas of potassic affinity³⁸, and distinctly different from that observed in the clinopyroxene, mica and amphibole of the Damodar Valley lamproites³⁹ and authors' unpublished data. The Rongjeng minerals are also chemically different from those observed in the Sung Valley carbonatitic–ijolitic intrusion⁴⁰.

The Primitive mantle normalized multi-element spidergrams of the Damodar Valley lamprophyres, eastern India Sylhet Traps and ultramafic lamprophyres from the Bea-

ver Lake, Antarctica are also compared with the studied Rongjeng potassic lamprophyre (Figure 8). It is observed that the sources of the nearby tholeiitic basalts of Sylhet and Rongjeng–Swangkre tholeiites must be chemically different, as pointed out by the distinct patterns and absolute abundances. The same can be noted for the contrasting geochemical patterns of the ultramafic lamprophyres in Antarctica, which were almost contemporaneously emplaced on the conjugate margin, and of the ultrapotassic rocks of the Damodar Valley, which also show negative Nb, Ta and Ti troughs resembling a crustally derived enrichment event in the mantle. The geochemical characteristics of the Rongjeng potassic lamprophyre are shared with other K-rich within plate basaltic-basanitic dyke suites, such as that in the Late Cretaceous magmatism of southeastern Brazil of the African Rift, among other examples⁴¹.

A simple mixing model between average compositions of depleted mantle melts (MORB) and melts derived from enriched sources (OIB) is presented in Figure 9. This simplistic model can be fruitful for the petrogenesis of the Sylhet traps and of the Rongjeng tholeiites, apart from likely effects of crustal contamination. Looking at the petrogenesis of the Rongjeng dyke to a regional scale, we note that the extreme trace element enrichment of the

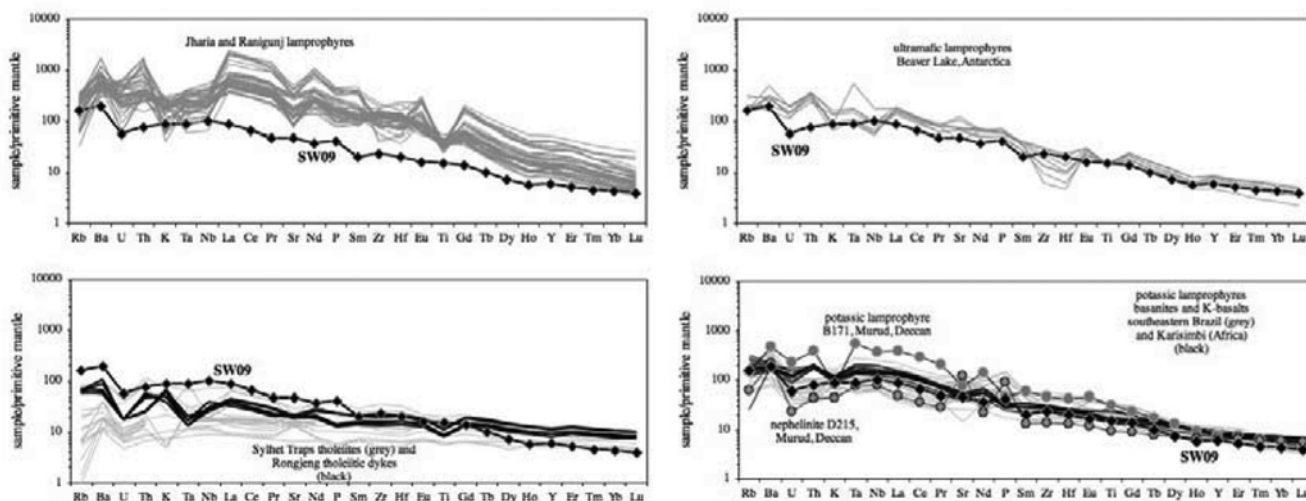


Figure 8. Primitive mantle normalized diagrams for mafic-ultramafic rocks and the studied Rongjeng potassic dyke (Data source (refs 17, 39, 41, 43–47)). The normalization values from Lyubetskaya and Korenaga⁴⁸.

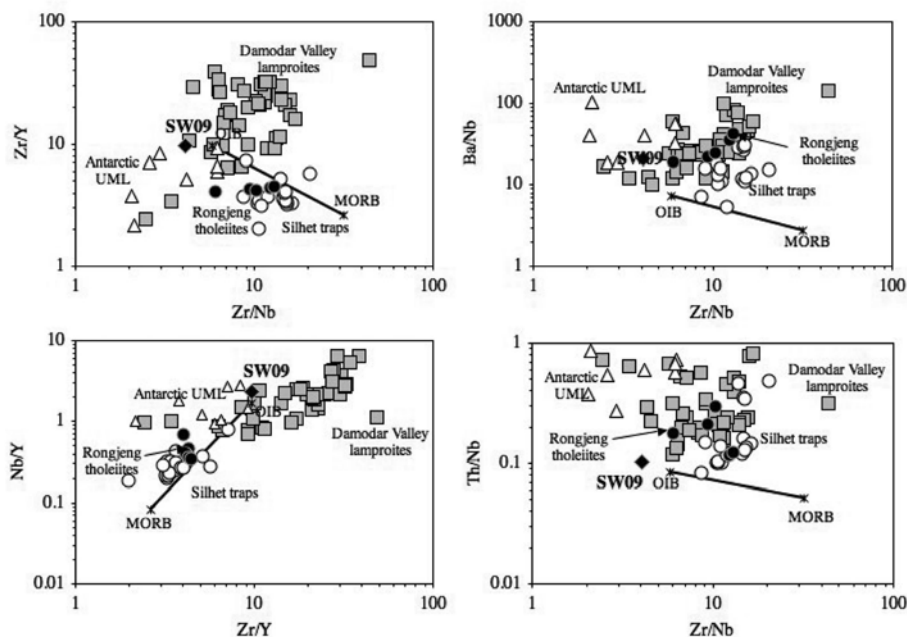


Figure 9. Incompatible element ratios of the Rongjeng potassic lamprophyre and other Cretaceous rocks from India, and Antarctica. The data are the same as in Figure 8. Trace element data for MORB and OIB are taken from Sun and McDonough⁴⁹.

Rongjeng dykes, the ultrapotassic rocks and the Antarctic ultramafic lamprophyres and their contrasting geochemical patterns cannot be due to input of plume-related magmatism of unknown composition, but, rather, to distinctive heterogeneity of the mantle source, which are typical of lithospheric alkaline magmatism.

Conclusions

Petrography, mineral chemistry and whole-rock geochemistry of an early Cretaceous, highly porphyritic lam-

prophyre sample from a dyke exposed near Rongjeng, East Garo Hills, Shillong plateau clearly suggest its potassic affinity. These features are typical of those crystallizing in hydrous alkaline magmas. Mineral chemistry of micas, pyroxenes and amphiboles is well comparable with the nearby Jasra potassic intrusion, and distinctly different from the Damodar Valley lamproites and the Sung Valley carbonatitic-ijolitic intrusion. The geochemical characteristics of the Rongjeng lamprophyre are very close to other K-rich within plate basaltic-basanitic dyke suites (Figure 8). A simple mixing model between

average compositions of depleted mantle melts (MORB) and melts derived from enriched sources (OIB) applied to the studied Rongjeng lamprophyre sample together with the Sylhet traps, the Rongjeng tholeiites, the ultrapotassic rocks, and the Antarctic ultramafic lamprophyres is suggestive of distinctive heterogeneity of the mantle source rather than input of plume-related magmatism; a typical situation of lithospheric alkaline magmatism.

1. Rock, N. M. S., The nature and origin of lamprophyres: an overview. In *Alkaline Igneous Rocks* (eds Fitton, J. G. and Upton, B. G. J.), Geol. Soc. London Spec. Publ., 1987, **30**, 191–226.
2. Woolley, A. R., Bergman, S. C., Edgar, A. D., Le Bas, M. J., Mitchell, R. H., Rock, N. M. S. and Scott-Smith, B. H., Classification of lamprophyres, lamproites, kimberlites, and the kalsilitic, melilitic and leucitic rocks. *Can. Mineral.*, 1996, **34**, 175–186.
3. Le Maitre, R. W., *Igneous Rocks: A Classification and Glossary of Terms*, Cambridge University Press, Cambridge, 2002.
4. Riley, T. R., Leat, P. T., Storey, B. C., Parkinson, I. J. and Millar, I. L., Ultramafic lamprophyres of the Ferrar large igneous province: evidence for a HIMU mantle component. *Lithos*, 2003, **66**, 63–76.
5. Tappe, S. *et al.*, Genesis of ultramafic lamprophyres and carbonatites at Aillik Bay, Labrador: a consequence of incipient lithospheric thinning beneath the North Atlantic Craton. *J. Petrol.*, 2006, **47**, 1261–1315.
6. Orejana, D., Villaseca, C., Billstrom, K. and Paterson, B. A., Petrogenesis of Permianalkaline lamprophyres and diabases from the Spanish central system and their geodynamic context within western Europe. *Contrib. Mineral. Petrol.*, 2008, **156**, 477–500.
7. Kerr, A. C., Khan, M., Mahoney, J. J., Nicholson, K. N. and Hall, C. M., Late Cretaceous alkaline sills of the south Tethyan suture zone, Pakistan: initial melts of the Réunion hotspot? *Lithos*, 2010, **117**, 161–171.
8. Srivastava, R. K. and Chalapathi Rao, N. V., Petrology, geochemistry and tectonic significance of Paleoproterozoic alkaline lamprophyres from the Jungel valley, Mahakoshal supracrustal belt, central India. *Mineral. Petrol.*, 2007, **89**, 189–215.
9. Chalapathi Rao, N. V., Precambrian alkaline potassic-ultrapotassic, mafic-ultramafic magmatism in Peninsular India. *J. Geol. Soc. India*, 2008, **72**, 57–82.
10. Chalapathi Rao, N. V., Dharma Rao, C. V. and Das, S., Petrogenesis of lamprophyres from Chhota Udepur area, Narmada rift zone, and its relation to Deccan magmatism. *J. Asian Earth Sci.*, 2012, **45**, 24–39.
11. Srivastava, R. K., Petrological and geochemical characteristics of Paleoproterozoic ultramafic lamprophyres and carbonatites from the Chitrangi region, Mahakoshal supracrustal belt, central India. *J. Earth Syst. Sci.*, 2013, **122**, 759–776.
12. Mallikharjuna Rao, J., Poornachandra Rao, G. V. S. and Sarma, K. P., Precambrian Mafic magmatism of Shillong Plateau, Meghalaya and their Evolutionary History. *J. Geol. Soc. India*, 2009, **73**, 143–152.
13. Sunilkumar, Dhanaraju, R., Varma, H. M. and Dougall, N. K., Cancrinite-tinguaite and K-rich trachyte in Nongchram–Darugiri area of East Garo Hills district, Meghalaya: a preliminary study. *J. Geol. Soc. India*, 1984, **25**, 528–533.
14. Nambiar, A. R. and Golani, P. R., A new find of carbonatite from Meghalaya. *Curr. Sci.*, 1985, **54**, 281–282.
15. Nambiar, A. R., Alkaline magmatism in parts of East Garo Hills and West Khasi Hills districts, Meghalaya. *Rec. Geol. Surv. India*, 1987, **115**, 25–41.
16. Nambiar, A. R., Petrology of lamprophyres from parts of East Garo Hills and West Khasi Hills districts, Meghalaya. *J. Geol. Soc. India*, 1988, **32**, 125–136.
17. Srivastava, R. K. and Sinha, A. K., Geochemistry and petrogenesis of early Cretaceous sub-alkaline mafic dykes from Swangkre-Rongmil, East Garo Hills, Shillong plateau, Northeast India. *J. Earth Syst. Sci.*, 2004, **113**, 683–697.
18. Srivastava, R. K. and Sinha, A. K., The Early Cretaceous Sung Valley ultramafic-alkaline-carbonatite complex, Shillong Plateau, Northeastern India: petrological and genetic significance. *Mineral. Petrol.*, 2004, **80**, 241–263.
19. Evans, P., The tectonic framework of Assam. *J. Geol. Soc. India*, 1964, **5**, 80–96.
20. Desikachar, S. V., A review of the tectonic and geological history of eastern India in terms of plate tectonic theory. *J. Geol. Soc. India*, 1974, **15**, 137–149.
21. Nandy, D. R., Tectonic patterns in northeastern India. *Indian J. Earth Sci.*, 1980, **7**, 103–107.
22. Gupta, R. P. and Sen, A. K., Imprints of Ninety-East Ridge in the Shillong Plateau, Indian Shield. *Tectonophysics*, 1988, **154**, 335–341.
23. Kumar, D., Mamallan, R. and Dwivedy, K. K., Carbonatite magmatism in northeast India. *J. Southeast Asian Earth Sci.*, 1996, **13**, 145–158.
24. Majumdar, S. K., A summary of the Precambrian geology of the Khasi Hills, Meghalaya. *Geol. Surv. India Misc. Publ.*, 1976, **23**, 311–334.
25. Das Gupta, A. B. and Biswas, A. K., *Geology of Assam*, Text Book Series, Geological Society of India, Bangalore, 2000.
26. Ghosh, S., Chakrabarty, S., Paul, D. K., Bhalla, J. K., Bishui, P. K. and Gupta, S. N., New Rb–Sr isotopic ages and geochemistry of granitoids from Meghalaya and their significance in middle to late Proterozoic crustal evolution. *Indian Min.*, 1994, **48**, 33–44.
27. Storey, M. *et al.*, Lower Cretaceous volcanic rocks on continental margins and their relationship to the Kerguelen Plateau. In *Proceedings of the Ocean Drilling Program, Science Results* (eds Wise, S. W. Jr. *et al.*), 1992, vol. 120, pp. 33–47.
28. Kent, R. W., Saunders, A. D., Kempton, P. D. and Ghose, N. C., Rajmahal basalts, eastern India: mantle sources and melt distribution at a volcanic rifted margin. In *Large Igneous Provinces: Continental, Oceanic and Planetary Flood Volcanism* (eds Mahoney, J. J. and Coffin, M. F.), AGU Mongraph, 1997, vol. 100, pp. 145–182.
29. Kent, R. W., Pringle, M. S., Müller, R. D., Saunders, A. D. and Ghose, N. C., $^{39}\text{Ar}/^{40}\text{Ar}$ geochronology of the Rajmahal basalts, India, and their relationships to the Kerguelen Plateau. *J. Petrol.*, 2002, **43**, 1141–1155.
30. Srivastava, R. K., Heaman, L. M., Sinha, A. K. and Shihua, S., Emplacement age and isotope geochemistry of Sung Valley alkaline-carbonatite complex, Shillong Plateau, northeastern India: implications for primary carbonate melt and genesis of the associated silicate rocks. *Lithos*, 2005, **81**, 33–54.
31. Srivastava, R. K. and Sinha, A. K., Nd and Sr isotope systematics and geochemistry of a plume-related Early Cretaceous alkaline-mafic-ultramafic igneous complex from Jasra, Shillong Plateau, northeastern India. *Geol. Soc. America Spec. Pap.*, 2007, **430**, 815–830.
32. Sarkar, A., Datta, A. K., Poddar, B. K., Bhattacharyya, B. K., Kollapuri, V. K. and Sanwal, R., Geochronological studies of Mesozoic igneous rocks from eastern India. *J. Southeast Asian Earth Sci.*, 1996, **13**, 77–81.
33. Roeder, P. L. and Emslie, R. F., Olivine-liquid equilibrium. *Contrib. Mineral. Petrol.*, 1970, **29**, 275–289.
34. Verma, S. P., Torres-Alvarado, I. S. and Sítelo-Rodríguez, Z. T., SINCLAS: Standard igneous norm and volcanic rock classification system. *Computer Geosci.*, 2002, **28**, 711–715.
35. Rock, N. M. S., The nature and origin of ultramafic lamprophyres: Alnöites and allied rocks. *J. Petrol.*, 1986, **27**, 155–196.
36. Rock, N. M. S., *Lamprophyres*, Blackie & Sons Ltd., Glasgow, 1991.

RESEARCH ARTICLES

37. Tappe, S., Foley, S. F., Jenner, G. A. and Kjarsgaard, B. A., Integrating ultramafic lamprophyres into the IUGS classification of igneous rocks: Rational and implications. *J. Petrol.*, 2005, **46**, 1893–1900.
38. Melluso, L., Srivastava, R. K., Petrone, C. M., Guarino, V. and Sinha, A. K., Mineralogy, magmatic affinity and evolution of the Early Cretaceous alkaline complex of Jasra, Shillong Plateau, northeastern India. *Min. Mag.*, 2012, **76**, 1099–1117.
39. Chalapathi Rao, N. V., Srivastava, R. K., Sinha, A. K. and Ravikant, V., Petrogenesis of Kerguelen mantle plume-linked Early Cretaceous ultrapotassic lamprophyres with affinities to lamproites from the Gondwana sedimentary basins, Damodar Valley, Eastern India. *Earth Sci. Rev.*, 2014, **136**, 96–120.
40. Melluso, L., Srivastava, R. K., Guarino, V., Zanetti, A. and Sinha, A. K., Mineral compositions and magmatic evolution of the Sung Valley ultramafic-alkaline-carbonatitic complex (NE India). *Can. Mineral.*, 2010, **48**, 205–229.
41. Brotzu, P., Melluso, L., d'Amelio, F. and Lustrino, M., Mafic/ultramafic dykes and felsic intrusions with potassic to ultrapotassic affinity in the Serra do Mar province: a review. In *Mesozoic to Cenozoic Alkaline Magmatism in the Brazilian Platform* (eds Comin-Chiaromonte, P. and Gomes, C. B.), FAPESP, São Paulo, 2005, pp. 443–472.
42. Irvine, T. N. and Baragar, W. R. A., A guide to chemical classification of the common volcanic rocks. *Can. J. Earth Sci.*, 1971, **8**, 523–548.
43. Srivastava, R. K., Chalapathi Rao, N. V. and Sinha, A. K., Cretaceous potassic intrusives with affinities to aillikites from Jharia area: Magmatic expression of metasomatically veined and thinned lithospheric mantle beneath Singhbhum Craton, Eastern India. *Lithos*, 2009, **112S**, 407–418.
44. Ghatak, A. and Basu, A. R., Vestiges of the Kerguelen plume in the Sylhet Traps, northeastern India. *Earth Planet. Sci. Lett.*, 2011, **308**, 52–64.
45. Andronikov, A. V. and Foley, S. F., Trace element and Nd–Sr isotopic composition of ultramafic lamprophyres from the East Antarctic Beaver Lake area. *Chem. Geol.*, 2001, **175**, 291–305.
46. Melluso, L., Sethna, S. F., D'Antonio, M., Javeri, P. and Bennio, L., Geochemistry and petrogenesis of sodic and potassic mafic alkaline rocks in the Deccan Volcanic province, Mumbai area (India). *Mineral. Petrol.*, 2002, **74**, 236–254.
47. Rogers, N. W., De Mulder, M. and Hawkesworth, C. J., An enriched mantle source for potassic basanites: evidence from Kari-simbi volcano, Virunga volcanic province, Rwanda. *Contrib. Mineral. Petrol.*, 1992, **111**, 543–556.
48. Lyubetskaya, T. and Korenaga, J., Chemical composition of Earth's primitive mantle and its variance: 1 Method and results. *J. Geophys. Res.*, 2007, **112**, 1–21.
49. Sun, S. S. and McDonough, W. F., Chemical and isotopic systematics of oceanic basalts: implications for mantle composition and process. In *Magmatism in the Ocean Basins* (eds Saunders, A. D. and Norry, M. J.), Geol. Soc. Spec. Publ. 42, 1989, pp. 313–345.

ACKNOWLEDGEMENTS. We thank Roberto de' Gennaro for his assistance in the microprobe work and Sergio Bravi for performing thin sections. This work has been partially supported by MIUR (COFIN 20107ESMX9-001) grants to L. Melluso and CSIR, New Delhi (Scheme No. 24(0251)/01/EMR-II) grants to R.K.S. We also thank N. V. Chalapathi Rao and an anonymous reviewer for their useful comments.

Received 9 September 2015; revised accepted 16 November 2015

doi: 10.18520/cs/v110/i4/649-658
